

Thick films of ceramic, superconducting, and electro-ceramic materials*

H. Altenburg^{1,2,‡}, J. Plewa², G. Plesch³, and O. Shpotyuk⁴

¹FH Münster/University of Applied Sciences, Lab. Supraleitung-Keramik-Kristalle (SKK), Steinfurt, Germany; ²SIMa, Steinfurter Initiative für Materialforschung, Steinfurt, Germany; ³Comenius University, Faculty of Natural Sciences, Department of Inorganic Chemistry, 842 15 Bratislava, Slovakia; ⁴Scientific Research Company “Carat”, Institute of Materials, Lviv, Ukraine

Abstract: The use of thick films becomes more and more important in particular for electronic and microelectronic applications. The term “thick film” does not relate so much to the thickness of the film but more to the kind of deposition. Thick films are made by low-priced processes such as doctor (dr) blading, screen-printing, or spraying methods, etc. The preparation of thick films of ceramic material by these methods generally implies a processing sequence of the following steps: preparation of the oxide powders; preparation of pastes and slurries; painting/printing, etc. of the pastes onto a suitable substrate; drying at low temperature; and sintering at high temperature to get a consolidated layer. These technologies and the fabricated thick films of thermoresistive and superconducting materials will be discussed.

INTRODUCTION

Thick-film technology is widely used for a variety of technological and commercial applications as wear, corrosion, and high-temperature-resistant coatings or with special functions for use in electronics, microelectronics, optics, and chemistry, etc. The development of thick-film negative temperature coefficient of resistance (NTC) thermistors and superconducting thick films was essential for the growth of the electronics industries in both of these fields and will be discussed here.

The types of material used for coatings can be ceramic materials on the basis of some classes of inorganic compounds such as oxides, carbides, and nitrides. In selecting the coating material, the matched substrate has to fulfill several conditions, such as no chemical reaction with the coating; no or minimal interdiffusion; or minimal thermal stress by matched thermal coefficient, providing good coating, surface adhesion, etc.

In the literature, one finds values for thicknesses of “thick films” that start with nanometers and go up to millimeters; normally, one finds 10–200 μm values, sometimes the values extend to mm. While thin films are usually prepared by methods such as chemical vapor deposition, sputtering, or laser ablation (which enforce epitaxial deposition on single-crystal substrates), thick films are made by low-priced processes such as doctor blading or screen-printing technologies with high productivity and reliability (see scheme in Fig. 1 printed by bold type in oval brackets [1]).

*Lecture presented at the 5th Conference on Solid State Chemistry (SSC 2002), Bratislava, Slovakia, 7–12 July 2002. Other presentations are published in this issue, pp. 2083–2168.

[‡]Corresponding author: E-mail: h.altenburg@fh-muenster.de

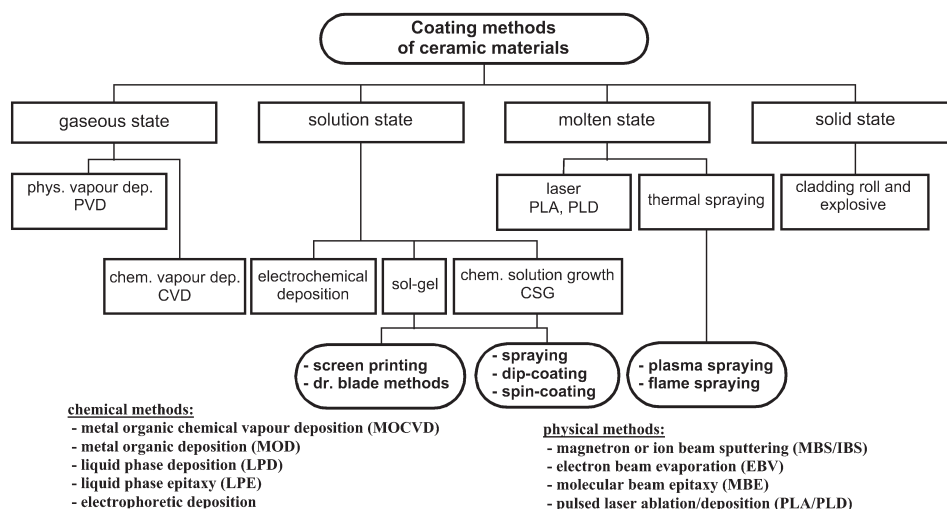


Fig. 1 Physical and chemical coating methods for thin and thick films.

THICK-FILM AND MATERIALS PREPARATION

Coating methods

Doctor blading

Doctor blading or tape casting is an economical method for producing large surface areas of ceramic films, which is very well suited for laboratory work and consists of printing, coating, or spreading paste with a blade onto a substrate (Fig. 2). In an industrial tape-coating process, a homogeneous, thoroughly dispersed concentrated slurry of ceramic material and organic polymer additives is applied to a temporary support with a dr blade [2]. After drying, the layer organic components still remain in the tape and must be removed by pyrolysis. The burning out of organic components generates open pores, which are eliminated by sintering.

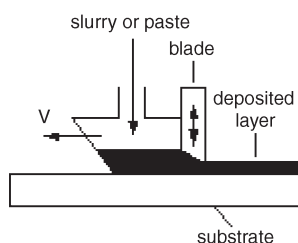


Fig. 2 Doctor blade method.

Screen printing

In the electronics industry, screen printing has been the dominant process for thick-film deposition. Since the end of the 1960s, several screen-printing models have been developed [3–5].

The advantages of screen printing are: high and precise line resolution, fast processing, and economical use of paste, thus leading to low costs [4]. In electronics, the liquids to be transferred differ from normal inks because usually they are mixtures of solid materials suspended in liquid vehicles such as organic solutions. The composition of such pastes or slurries is important for successfully achieving the printing and the following firing steps.

Screen printing simulates an extrusion process, since the liquid is first forced into the open areas of a patterned screen and then transferred to the substrate [5]. This is done by moving an excess of slurry across the patterned screen in front of a squeegee blade, which presses down the screen (Fig. 3).

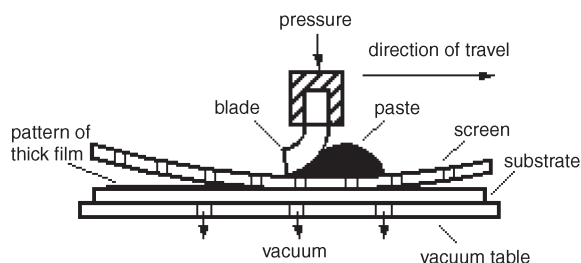


Fig. 3 Screen-printing machine for thick films.

Spraying and spin and dip coating

Spraying and dip-coating methods are very well known in the metals, plastics, and varnish industry. Dip coating is a stationary batch process, by which a substrate is dipped into a solution, slurry, or paste. In spin coating, in order to deposit very thick films, one side of a substrate is coated by dripping the solution onto the center of a substrate that is rotating at high speed. This step must be repeated several times in order to achieve the required thickness [6].

Thermal spraying

Spraying molten materials onto a cold adhesive support may be done by flame spraying (3200 °C), powder spraying (3200 °C), arc spraying (5500 °C), or ore plasma spraying (20 000 °C), which essentially differ as to how energy is generated [7]. Which method is to be applied depends on the kind of material to be sprayed and on the level of spraying performance required. Apart from metals, mainly oxides, but also carbides, nitrides, and borides are used. The work piece to be treated may be very large, can have any shape, and is hardly warmed up during processing. For particularly high-melting inorganic materials, a plasma burner (Fig. 4), which can attain ten times higher temperatures, is better suited. A gas-stabilized electric arc ionizes the gases (e.g., argon, helium, or nitrogen), which are introduced into a high-energy plasma. The explosion-like expansion of the gaseous plasma imparts high energy to the gas particles, which are expelled through the nozzle at high velocities.

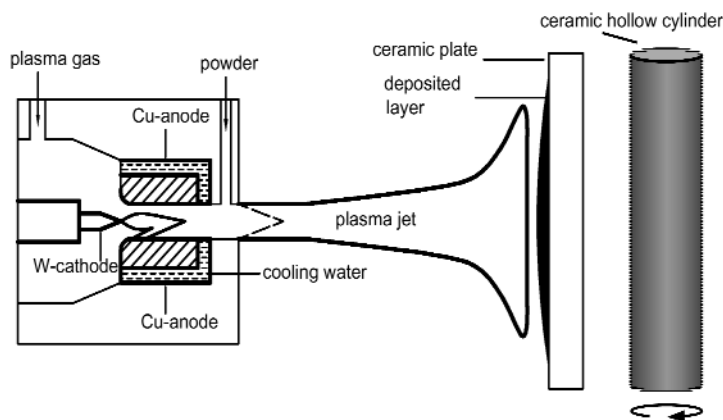


Fig. 4 Plasma spraying.

The coating material (which is usually powdered) is melted, accelerated, and hits the work piece to be coated with high kinetic energy. The advantage of the plasma process lies in the build-up of layers of various thickness and good adhesion. A special process allows spraying of very thick rigid “layers” (about 80 mm) onto a reusable core part [8].

Coating pretreatment

Powder preparation

The quality of the initial powder material is a crucial point in processing ceramic work pieces. This is the reason why so many investigations have been carried out on how to prepare tailored powders in terms of purity, homogeneity, reactivity, grain size, and grain distribution. The simplest customary method of oxide powder preparation is the traditional “ceramic” method, i.e., mixing and firing of oxides, carbonates, or nitrates of the components according to the required stoichiometry. Specific precursor routes such as “reactive mixtures” or the “flakes method” [9] have been tested on the occasion of superconductor preparation [10]. Solution chemistry solves much better all these problems concerning agglomeration, grain sizes, and distribution ranges and leads to active, homogeneous fine-grain powders. There are two main kinds of powder preparation by wet chemistry—the coprecipitation method and the sol-gel process. Freeze drying and spray drying, for example, are specific follow-up methods for obtaining powders.

Paste/slurry preparation

The paste/slurry preparation comprises, apart from the ceramic powders, a variety of organic additives; thus, pastes and slurries represent multicomponent and complex systems. The additives include solvents and binders as well as plasticizers, homogenizers, sometimes dispersants/deflocculants, and inorganic grain growth inhibitors.

Solvents can either be aqueous (thus, inexpensive), incombustible, and nontoxic or nonaqueous of low viscosity, low boiling point, low evaporation heat, and high vapor pressure. Nonaqueous systems are used for high-performance materials and are commonly highly polar organic compounds such as alcohols, ketones, hydrogenated hydrocarbons, and mixtures of them. For solubility reasons, it is customary to apply two solvents. Frequently, azeotropic mixtures (e.g., trichloroethylene/ethanol [2]) are used.

The main function of the binder is to establish adhesion of the ceramic green tape after the solvent has been evaporated, and this adhesion should assure good tape handling, yet without leading to the formation of cracks and defects. Polyvinyl-butyril (PVB) is a commonly used binder, which is soluble in nonpolar media, acts as a dispersant, and decomposes slowly during the burn-out period.

Plasticizers are added to complement the binder; they improve the flexibility and workability of the green tape by reducing the glass-transition temperature. PVB is usually plastified by glycols (polyethylene-glycol, PEG) and/or by phthalates and acrylic binder by dimethyl- or benzyl-butyl-phthalate.

Sol-gel

The term “sol-gel” describes a type of process in which a colloid solution—the sol—is converted into a gel with solid-like properties [11]. The starting material is a salt that is converted either by hydrolysis in a colloidal polyvalent metal ion like $\{[\text{AlO}_4\text{Al}_{12}(\text{OH})_{24}(\text{H}_2\text{O})_{12}]\}^{7+}$, thereafter by peptization into a sol, or by alcoholysis into the most interesting alkoxides (MeOR). The hydrolysis of a zirconium alkoxide $\text{Zr}(\text{OR})_4$ leads to a sol containing different polymers finely dispersed in the solution.

Slight evaporation gives rise to aggregation or polymerization, resulting in an interconnected “solid” network having an interspersed continuous liquid phase—the so-called “gel”. Thermal treatment yields the inorganic ceramic oxide. Hydrolysis of alkoxides has been used to prepare several oxides of Al, Fe, Ti, or Si, etc., mostly as powders, but it may also be used for obtaining fibers and coatings. The techniques for making sol-gel coatings are dipping, spinning, and spraying as described in ref. [12].

Substrates

In electronics, substrates serve as support materials, which other materials with different properties are coated onto in order to create electrical devices or circuits. Favorite materials are aluminum oxide-based ceramics. For example, Al_2O_3 is used as a substrate in silicon on sapphire (SOS) technology or for thick-film NTC thermistors. Apart from other properties, it is highly resistant to alternating temperatures and shows low dielectric losses. In addition, aluminum nitride-based ceramics and beryllium oxide are used as materials of high thermal conductivity. Cordierite, mullite, SiC, or metalized substrates are used less commonly. Specifications concerning these materials and their use have been published [13].

Oxide single crystals, ceramics, and metals and/or alloys have been tested as to their suitability for serving as substrate materials for superconducting thick and thin layers. Sufficient chemical and thermal stability are key properties of a substrate, i.e., it may not react chemically with the coating.

Numerous substrate materials, which in thin-film technology can often only be used in combination with buffer layers, cannot at all be used in thick-film fabrication because of the high sintering temperatures of 900–1100 °C (YBCO) and of 800–950 °C (BSCCO). This is particularly true for Si and SiO_2 as well as for Al_2O_3 , but less so for sapphire, MgO, and various aluminates [14]. Koshy, John et al. [15] found out that the perovskite-like structures of niobates and hafnates having the formulas $(\text{RE})\text{Ba}_2\text{NbO}_6$ and $(\text{RE})\text{Ba}_2\text{HfO}_{5.5}$ (RE = rare earth) are candidates for substrates. Superconducting YBCO and Bi-2223 do not show any detectable chemical reaction with, for example, $\text{LaBa}_2\text{HfO}_{5.5}$ even under extreme processing conditions. For electronic applications, a low dielectric constant ($\epsilon < 20$) and low microwave losses ($\tan \delta < 10^{-3}$) are required. SrTiO_3 (ideal as a thin-film substrate), due to its very high electronic values, is out of question for use in electronics. MgO, which is commercially available, and polycrystalline YSZ are preferred, although the latter exhibits less-useful electronic values. Insofar as the electronic values are concerned, these two conventional substances may be compared with the potential substrate candidates niobates and hafnates.

Sintering

“Sintering” is used to describe the consolidation of a product by heating just below the melting point. Solid-state sintering, which involves only solid phases, is traditionally used for ceramic powders with melting points between 1300–2000 °C. Examples are a crystalline single phase such as $\alpha\text{-Al}_2\text{O}_3$ or a single phase containing dopant materials such as Al_2O_3 with 0.5 % MgO, ZrO_2 with 3 % Y_2O_3 , or SiC with 2 % B_4C .

Finely grained powders and suitable doping materials lower the sintering time and temperature and yield a better densification. Liquid-phase sintering takes place when a liquid phase coexists with solid phases and plays an important role in the processing of ceramics.

The liquid phase spreads and wets the particles, which causes particle rearrangement through capillary forces and grain boundary diffusion. The liquid phases resulting from addition of fluxing agents (low melting point), like borosilicates or glassy phases distributed in the grain boundaries, etc., strengthen drastically the effect of densification [16]. Liquid-phase sintering processes have been widely used to prepare high-temperature superconducting (HTSC)-ceramics too [17]. But these processes do not exactly follow the conventional route. Chemical reactions between the stoichiometric precursor components occurring at lower temperatures result in the formation of the liquid phase (partial melting), and these phases are very important for the formation of the textured microstructure. Several sintering regimes have been developed for bulk and thick films for such materials as YBCO and BSCCO (Fig. 7).

NEW NEGATIVE TEMPERATURE COEFFICIENT ELECTROCERAMIC THICK FILMS

Thick-film NTC thermistors are widely used in the various fields of modern electronics such as thermal stabilization and compensation, temperature measuring and control, etc. [18]. For example, thick-film

temperature sensors (chips, bridges, average temperature sensors, model plates to measure surface thermal conduction of fluids, and so on) are characterized by high yield, high accuracy, reliability, and interchangeability attained by functional trimming. Hybridization of these sensors with resistors allows one to attain twice the sensitivity. Application of hybrid microelectronic circuits containing thick-film NTC thermistors (vertical output module for TV, semiconductor strain gauge for a pressure transmitter, pressure sensors for automobiles) leads to considerable cost reduction and miniaturization of the sensing systems. Quite reliable and stable thick-film elements can be prepared from transition-metal oxides by traditional printing technologies, however, they possess a comparatively narrow range of electrical parameters.

It is possible to remove this disadvantage using more complex semiconducting spinel-based electroceramics within the $\text{NiMn}_2\text{O}_4\text{--CuMn}_2\text{O}_4\text{--MnCo}_2\text{O}_4$ system [19,20]. Using these ceramics in conjunction with proper printing technology results in highly stable thick-film NTC thermistors with good electrical resistance R and thermistor constant B at a level not inferior to that encountered in the analogous bulk ceramics. $\text{Cu}_{0.1}\text{Ni}_{0.1}\text{Mn}_{1.2}\text{Co}_{1.6}\text{O}_4$ -based thick films can be taken as good examples for demonstration.

The paste needed for thick-film printing is prepared by mixing previously powdered ("Fritsch" drum mill) $\text{Cu}_{0.1}\text{Ni}_{0.1}\text{Mn}_{1.2}\text{Co}_{1.6}\text{O}_4$ ceramics together with organic (ethylcellulose dissolved in terpenol) and inorganic (glass) binders. The final grain sizes in this powder do not exceed $5\ \mu\text{m}$. This paste contains as high as 75.76 % $\text{Cu}_{0.1}\text{Ni}_{0.1}\text{Mn}_{1.2}\text{Co}_{1.6}\text{O}_4$ powder, 18.94 % organic solvent and binder, and 5.3 % glass powder with Bi_2O_3 . The paste obtained is deposited onto Al_2O_3 (Rubalit 708S) substrates with preliminarily applied silver contacts, using traditional screen-printing technique (DFS-0,1 device, equipped with steel screen). These films are then annealed in conveyer furnace BTU (slow temperature rise up to 1120 K, isothermal shelf for 15 min and quenching down to room temperature). After annealing, thick films have the following chemical composition: 93.5 % $\text{Cu}_{0.1}\text{Ni}_{0.1}\text{Mn}_{1.2}\text{Co}_{1.6}\text{O}_4$ ceramics, 2.8 % Bi_2O_3 , and 3.7 % HT-521-4 glass. The above technological route allows one to obtain both the single- ($50\text{--}70\ \mu\text{m}$) and double-layered ($100\text{--}150\ \mu\text{m}$) plane-type thick-film NTC thermistors.

It is established by optical microscopy that the thick-film NTC thermistors show good morphologies, high densities, and sufficiently smooth surfaces. They contain uniformly distributed grains ($<4\ \mu\text{m}$ in diameter), embedded into the glass phase. X-ray diffraction studies show that the prepared films have a typical spinel structure. The temperature dependence of resistivity of the thick films (Fig. 5) is described by a well-known expression valid for NTC thermistors [18]:

$$R(T) = R_{298} \times \exp(B/T - B/298) \quad (1)$$

The electrical resistivity of $2 \times 50\ \mu\text{m}^2$ surface area of single-layered thick film is approximately 350 k Ω , while the thermistor constant B for single- and double-layered samples is $3630 \pm 5\ \text{K}$, compared to $3530 \pm 5\ \text{K}$ for the analogous bulk specimen.

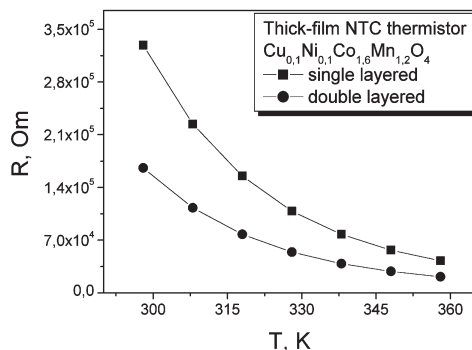


Fig. 5 Temperature dependencies of resistance for the investigated thick-film NTC thermistors.

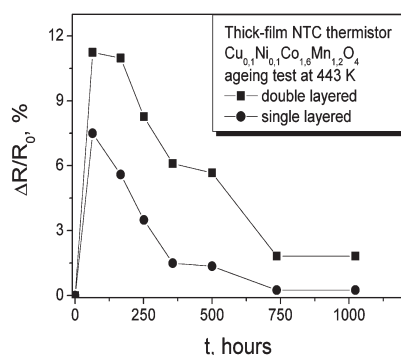


Fig. 6 Time dependence of relative resistance change ($T = 443$ K) in the obtained thick-film NTC thermistors.

The degradation tests at $T = 443$ K shows that electrical resistivity of the $\text{Cu}_{0.1}\text{Ni}_{0.1}\text{Mn}_{1.2}\text{Co}_{1.6}\text{O}_4$ -based thick-film thermistors first increases on thermal exposition and subsequently decreases as a function of time (Fig. 6). This decrease (the so-called “fatigue” effect in aging) has been observed for the first for this type of films. This anomalous behavior of thermal degradation kinetics is supposed to be associated with incomplete formation of intergranular boundaries in the thick film.

Thus, in such a way, the structurally uniform thick-film $\text{Cu}_{0.1}\text{Ni}_{0.1}\text{Mn}_{1.2}\text{Co}_{1.6}\text{O}_4$ -based NTC thermistors, which possess the high value of thermistor constant B and time-stable electrical parameters, can be manufactured for broad multifunctional device application in electronics.

HIGH-TEMPERATURE SUPERCONDUCTORS

HTSC thick films of the systems YBaCuO , Bi(Pb)SrCaCuO , and TlBaCaCuO are, besides some others, the most investigated materials (Table 1). Liquid melt-processed bulk materials are highly perspective

Table 1 T_c values of some superconductors.

Material	Chemical compounds and phases	T_c [K]	
1. Metals	Hg	4.15	
	Pb	7.2	
	Nb	9.2	
2. Alloys	V_3Si	17.1	
	Nb_3Sn	18.0	
	Nb_3Ge	23.2	
3. Cuprates (HTSC)	YBCO 123	$\text{YBa}_2\text{Cu}_3\text{O}_{7-x}$	92
	YBCO 124	$\text{YBa}_2\text{Cu}_4\text{O}_8$	80
	BSCCO 2212	$\text{Bi}_2\text{Sr}_2\text{CaCu}_2\text{O}_{8+x}$	92
	BSCCO 2223	$\text{Bi}_2\text{Sr}_2\text{Ca}_2\text{Cu}_3\text{O}_{10+x}$	110
	TBCCO 2212	$\text{Tl}_2\text{Ba}_2\text{CaCu}_2\text{O}_{8+x}$	105
	TBCCO 2223	$\text{Tl}_2\text{Ba}_2\text{Ca}_2\text{Cu}_3\text{O}_{8.5+x}$	125
	HBCCO 1212	$\text{HgBa}_2\text{CaCu}_2\text{O}_{5.5+x}$	122
	HBCCO 1223	$\text{HgBa}_2\text{Ca}_2\text{Cu}_3\text{O}_{8.5+x}$	135
4. Organic compounds	$(\text{BEDT-TTF})_2\text{Cu}(\text{CNS})_2$	11.1	
5. Fullerenes	K_3C_{60}	19.3	
	Rb_3C_{60}	30.0	
6. Borides	MgB_2	36.6	

for use in outer magnetic fields, e.g., for magnets (single domain material) with transport current densities in the range $j_c = 10^4$ – 10^5 A/cm². On the other hand, epitaxial films on the single-crystal substrates used in microelectronics show values about 10^6 A/cm² (77 K, 0 T). Melt-processed thick films, above all on polycrystalline substrates, are about the best compromise between the properties of bulk ceramics and epitaxial thin films.

YBCO thick films

Silver, partially some silver alloys or nickel and its alloys, does not show any substantial reaction with YBCO or the other HTSC-compounds, so these metals are often used as substrate materials.

Investigation of RABiTS (rolling assisted biaxially textured substrates) and IBAD (ion beam-assisted deposition) processes have demonstrated that YBCO can be deposited on textured metal-substrates with good current densities of about 10^5 – 10^6 A/cm². But both processes need PVD techniques not easily comparable with the low-cost attractive thick-film coating techniques.

Doctor blading and screen printing

It has been shown that improved properties can be achieved in YBCO thick films by employing the dr blade and screen-printing method and a processing regime that includes heating the YBCO above the peritectic temperature. The observed current densities in melt-processed thick films are significantly greater than in those produced by sintering in absence of a liquid phase. The peritectic reaction observed on heating YBCO involves the decomposition of $\text{YBa}_2\text{Cu}_3\text{O}_{7-x}$ (123) to form Y_2BaCuO_5 (211) and a Ba/Cu-rich liquid phase, which is highly corrosive [21]. Several substrates, such as Al_2O_3 , even with buffer layers, are not suitable because of reaction with the superconducting film.

Rangel et al. [22] produced polycrystalline thick films of silver-doped YBCO by a screen-printing ceramic method on single-crystal MgO-substrates. After electron irradiation with a dose rate of 25 kGy/min for a total dose of 1000 kGy, the current density increased by a factor 6.6 in comparison to the nonirradiated YBCO/Ag probes. The value of $j_c = 2.6 \times 10^6$ A/cm² estimated from the width of measured hysteresis loops by means of the Bean model is one of the highest for thick films and demonstrated the combined effect of metal addition and electron irradiation.

However, rhodium, palladium, and particularly platinum additions can greatly improve the superconducting properties; in particular j_c characteristics in melt-processed YBCO thick films (mainly) on YSZ substrate. By addition of 0.1 wt % Pt-powder, the critical current density increased, for example, from 2×10^3 A/cm² to 5×10^3 A/cm² and dropped down to nearly zero by addition of 0.2 wt % Pt [23].

Ingle et al. show a further interesting effect. The microstructure at the melt-processed YBCO films display a characteristic spherulitic morphology, which was described as the “hub and spoke” of a bicycle wheel [24] and is dependent on the thickness of the film. The individual grains in thinner films grow with a “rosette”-like structure from a central core, the hub. Below a film thickness of about 50 μm , the radially grown grains or spokes are not connected with each other; above about 100 μm , the hub and spoke structure disappears. The calculated critical current densities show optimal values at a thickness of 53 μm (2×10^4 A/cm²) corresponding to the microstructure.

A solid–liquid melt growth (SLMG) and powder melt-process (PMP) route utilizes precursors consisting of BaCuO_2 –CuO flux mixed with Y_2O_3 or Y_2BaCuO_5 . By this way, Langhorn et al. [25] found bigger spherulite size (up to 15 mm) by processing thick films using prereacted YBCO material. The relative texturing and the current density increased from about 900 A/cm² (commercial YBCO) to 2200 A/cm² (SLMG powder).

Spraying method

The spraying method is one of the most convenient processes of preparing thick films using ultrafine powders. The technique is relatively simple and inexpensive and allows spraying on substrate independent of its form. The deposition rate is higher than that for the deposition by PVD vacuum methods, and the density is higher than that at films prepared by dr blading or screen printing. Schulz et al. [26]

sprayed a mixture of fine powdered YBCO and ethanol onto Ni and Ni-alloy substrates, and he has reported that the films of a thickness of 80–100 μm fired at 1000 °C retained zero resistivity up to 85 K. Yoshimura, Matsuoka, and Ban prepared and tested YBCO films (1.5–7 μm ; 70–80 μm) on Ni-alloys and Al_2O_3 and YSZ substrates with and without buffer layers [27,28].

Spray pyrolysis

Spray pyrolysis has been widely employed for production of powders, but also for film deposition. Films can be produced from acetate or other organic precursor solutions and from “carbon-free” nitrate solutions. Spray pyrolysis of YBCO films can be split up into low- (substrate temperature 200–400 °C) and higher-temperature processes (substrate temperature 500–800 °C). A subsequent sintering step is still required to get a sufficiently textured YBCO. As early as 1991, Jergel et al. [29] prepared YBCO “thin” films (1–10 μm) from aerosols by a low-temperature deposition process consisting of two steps. It was shown by MacManus-Driscoll et al. [30] that epitaxial film growth was possible with j_c about $1 \times 10^4 \text{ A/cm}^2$ (77 K, 0 T) by ultrasonic spray pyrolysis.

Spin and dip coating

Typical coated HTSC-conductors consist of a metal substrate coated with a buffer layer on which YBCO is deposited in form of a thick film. Sathyamurthy and Salama [31] applied metal-organic decomposition (MOD) techniques together with spin-coating methods to deposit buffer layers (BaZrO_3 and SrTiO_3) and then YBCO films (ca. 0.5 μm) onto SrTiO_3 and LaAlO_3 substrate and reached j_c values of 10^4 – 10^5 A/cm^2 .

Kurian et al. [32] discussed a very interesting dip-coating process developed on a polycrystalline new dysprosium barium niobate, $\text{DyBa}_2\text{NbO}_6$ (DBNO). The dip-coated YBCO and Bi-2223 thick films (~4 μm) had excellent adhesion onto the DBNO substrate and show j_c values of about $\sim 1.1 \times 10^4$ and $4 \times 10^3 \text{ A/cm}^2$.

Plasma-spraying methods

Plasma-spraying methods were tried for a preparation of YBCO thick films with sufficient current densities just after the discovery of HTSC. Only small j_c values were obtained like 690 A/cm^2 (Tachikowa, 1988), 300 A/cm^2 (Lugscheider, 1989), 460 A/cm^2 (Pawlowski, 1990), 200 A/cm^2 (Hemmes, 1993), and 145 A/cm^2 (Seigmann, 1999).

Plasma-spraying processes are low priced, and it is easy to prepare extended ceramic layers and complicated shapes having very good adhesive power. YBCO layers stick very well on polycrystalline or rough crystalline substrates, however, the reactivity toward all substrates is high. The other problem is the low density of the ceramic YBCO layer. To obtain films with good superconducting properties, substrates have to be coated several times. Improved superconducting properties can be obtained by deposition of additional HTSC layers prepared by paste, painting, or dr blading methods and by a consecutive treatment with laser irradiation [33,34].

BSCCO thick films

Thick films of BSCCO have been prepared with thicknesses in the range of 10 to 1000 μm by tape casting (dr blading, painting), screen printing, dip coating, and not-as-yet mentioned electrophoretic deposition (EPD), and two special kinds of BSCCO thick film fabrication methods, the PIT/OPIT-process (oxide-powder-in-tube) and the PAIR-process (pre-annealing intermediate rolling).

Powder-in-tube method

The most widely considered manufacturing method for superconductors in the form of wires and tapes is the BSCCO-OPIT-route for Bi-2223, respectively for 2212. The last one is more attractive for low-temperature and/or high magnetic field application, in spite of its lower critical transition temperature. First, a precursor is packed into a metal tube, typically made of Ag or Ag-alloys, and sealed to form a billet, which is transformed into a rather long monofilamentary wire. The single filaments are bundled

and again processed by extrusion to form a thin rod in which the single filaments have become even thinner and more resistant to crack formation. The BSCCO wires are then rolled down into a tape and are textured by a heat treatment at 800–900 °C. In the resulting multifilament composite structure, the fine superconducting filaments are embedded into a metal matrix. Keller [35] reported on the progress in wire and tape fabrication at Eucas Congress (2001). However, current densities between 10^4 – 10^5 A/cm² are discussed dependent of the microstructure, sintering [36], thickness, and of the influence of the outer magnetic field [37], etc.

PAIR process

The PAIR process is a new method to obtain Bi-2212/Ag multilayer tapes. A silver or AgMg-alloy tape (about 20 μm thick, 100 μm long) was coated with a slurry and laminated with a second Ag foil. The green tape was wound in a pancake shape, pre-annealed (840–960 °C, 10–30 h in O₂), and deformed by rolling with a reduction of thickness of 25–40 %. The process is performed by partial melting (<900 °C, about 10 min) and an annealing step (to 840 °C and then to ambient temperature). Tapes prepared in this way have dimensions of 0.15–0.20 μm thickness and about 5 mm in width and show current densities of 1.5 – 5.0×10^5 A/cm² (4.2 K, 0 T). Hasegawa et al. [38], for example, reported on a dip-coated PAIR-process with similar values, influenced by the carbon content, the thickness and length of the layer. Kitaguchi [39] discussed the influence of the magnetic field on j_c values at temperatures between 10–50 K.

Tape casting

Tape casting (dr blading, painting), in contrast to the processes above, is much simpler and does not require mechanical deformation. Buhl [40] and Lang [41] found a dependence between $j_c = 10^3$ – 10^4 A/cm² and the thickness of the layers (10–1000 μm), sintering temperatures, and the annealing time as well as the influence of the magnetic field [42]. Bi-2212 thick films on MgO-substrate showed the same good quality as such films on Ag-substrates [43]. The thermal processing of the laminated green BSCCO-tape (e.g., on MgO) is composed of six stages represented in Fig. 7.

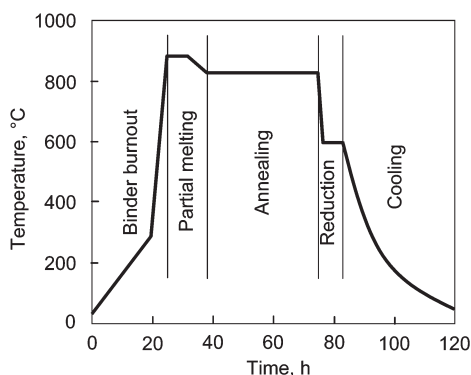


Fig. 7 Temperature profile for thermal processing of BSCCO thick films.

Screen printing and dip coating

Soon after the discovery of the BSCCO-substances, investigations were made to check whether screen-printing methods were suitable. Later on, Glowacki (2001) used an ink-jet printing method for a drop-wise deposition of a Bi-2212 slurry on Ag- and Mg-substrates [44]. Dip coating [45] allows the preparation of long tapes similar to those provided by the PIT or the PAIR process. A Bi-2212 layer (18–34 μm) sheathed from both sides by Ag foils, pressed and melted under controlled atmospheres [46], shows j_c values above 10^5 A/cm² at 4.2 K.

Electrophoretic deposition

EPD is a very interesting alternative approach to the fabrication of superconductor metal composites, which allows easy deposition of the oxides onto substrates of various shapes, including long wires, without organic residues being left in the coating after drying. The optimal partial melting temperature of Bi-2212 is 885 °C, the optimal annealing temperature is about 830 °C, and the optimal annealing time is above 60 h [47]. These conditions are favorable for the industrial manufacture of tape conductors with j_c values of 10^6 and 5×10^5 at 4.2 K (0 and 15 T).

Tl- and Hg-based high-temperature superconducting thick films

A great number of studies have been devoted to thick films of Tl- and Hg-based superconductors, for which critical temperatures are above 100 K. A comprehensive review until 1996 on Tl-based thick film has been published by Jergel et al. [48].

Doctor blading

Thick-film technologies, which use deposition of inks or slurry, can be applied to very simple and inexpensive continuous fabrication of wires and tapes. Kampwirth et al. [49] prepared Tl-1223 films with a thickness ranging from 10–50 μm on single crystals of MgO, YSZ, and silver. They used the two-step technique, i.e., in the first step they applied the ink of a Tl-free precursor, which was then thalliated in the second step in a Tl₂O atmosphere in a two-zone furnace. The superconducting films show some degree of orientation. The best superconducting properties showed the Sr- and Bi-containing samples, where T_c is 110 K and the transport critical current densities were 6800 A/cm² (77 K, 0 T). However, in magnetic fields, the films showed weak link behavior.

Screen printing

Screen printing was employed by Heiml et al. [50] to fabricate thin films of the composition (Tl_{0.6}Bi_{0.16}Pb_{0.24})(Ba_{0.1}Sr_{0.9})₂Ca₂Cu₃O_y with a thickness of 9–35 μm on silver-coated polycrystalline YSZ substrates. The paste was prepared from (Tl_{0.6}Bi_{0.16}Pb_{0.24})(Ba_{0.1}Sr_{0.9})₂Ca₂Cu₃O_y superconducting powders mixed with organic binder. The films were polycrystalline, however, their texture and also the transport critical currents can be improved by additional recompaction at 1 GPa and by follow-up annealing in oxygen atmosphere. The samples exhibited T_c values up to 118 K and transport critical currents 7.4×10^3 A/cm² (77 K, 0 T). Lee et al. [51] showed that the partial substitution of Ba for Sr in (Hg,Pb)-1223 thick films deposited by screen printing on polycrystalline MgO substrate significantly enhanced their chemical stability. The films showed T_c values of 120 K and transport critical current densities in order of 10^3 A/cm² (77 K, 0 T), indicating the presence of weak links on grain boundaries.

Dip coating

Thick films of the composition (Hg_{0.8}Re_{0.2})Ba₂CaCu₂O_{6+x}[(Hg,Re)-1212] were fabricated by a two-step method of dip coating and rolling the Re_{0.2}Ba₂CaCu₂O_{6+x} precursor onto a silver substrate [52]. The precursor tapes were then reacted in Hg vapor to yield films consisting of colonies of aligned dense grains. The film showed a T_c value of 118 K. It has been shown that the major contribution to critical current originates from the thin layer close to the interface with the substrate. The average value of critical current density is 3×10^3 A/cm² (4.2 K, 0 T). The results obtained until now show that the ink technologies are potential candidates for practical applications. However, it is still an open question whether this procedure will be able to produce also high-performance films.

Electrodeposition

Electrodeposition of superconductor tapes has considerable practical potential, particularly in the fabrication of large nonplanar devices and tapes on conductor or conductor-coated insulating substrates. It leads to high-quality films and tapes with thicknesses up to 15 μm . Bhattacharya et al. [53] deposited biaxially textured Tl-1223 films with a width of 1.6–2.6 μm on Ag-coated single crystal of LaAlO₃. The films were prepared by coelectrodeposition of Tl, Bi, Sr, Ba, Ca, Cu nitrates in dimethyl sulfoxide sol-

vent. Transport measurements of these films with $T_c = 110$ K showed values above 10^6 A/cm² (77 K, 0 T) which decreased to 10^3 A/cm² in outer magnetic fields (77 K, 3 T). Bellingeri et al. [54] prepared biaxially textured Tl-1223 on Ag tapes and Ag-coated SrTiO₃ single crystal by analogous techniques. The films where the final annealing was performed at high pressure of helium (50 bar) showed T_c values of 118 K.

Dip coating

Tsabba et al. [55] prepared Hg-1223 thick films substrate by depositing Ba, Ca, Cu nitrate gel in water–glycerol mixtures on polycrystalline YSZ. Spraying or dip coating was used as a deposition technique. The reaction of precursor films with mercury vapors in closed ampoules led to films with a T_c value of 135 K and a thickness of 5–10 μm. The magnetic measurements indicated critical current densities of about 5×10^3 A/cm².

Spray pyrolysis method

Sin et al. [56] prepared (HgRe)-1223 films on MgO monocrystalline substrates in a two-step process, wherein the Re, Ba, Ca, and Cu nitrates were deposited from aqueous solutions. After their calcination, the reaction with Hg vapors in closed vessel led to films with a T_c value of 133 K and a critical current density of 1×10^3 A/cm² (77 K, 0 T). Tl-1223 films, which were well aligned, were prepared on polycrystalline substrates by a spray pyrolysis deposition followed by a thalliation reaction in a two-zone furnace for exact control of a Tl vapor partial pressure. They showed j_c values of 6×10^4 A/cm² (77 K, 0 T) [57].

CONCLUSIONS

Coating methods, substrate and layer materials as well as processing with reference to NTC electroceramics and high T_c superconductors have been discussed. It was shown that NTC thermistor ceramics based on Mn/Co oxides can be prepared as thick films on Al₂O₃. In the field of HTSC, the three materials systems YBCO, BSCCO, and TBCCO have large potential for practical application. The preferred process for obtaining thick films, particularly on YSZ/MgO or Ag metal, consists of partial melting, solidification, and annealing. It was demonstrated that dr blading and screen-printing methods yield samples with improved properties. PIT and PAIR methods are most suited for BSCCO processing. The microstructures and thus the weak links between the superconducting grains, which are crucial for current densities, are dependent on the substrate–film interaction, thickness of the films, sintering and annealing temperatures, and processing time and atmosphere.

ACKNOWLEDGMENTS

The authors gratefully acknowledge support from the Deutsche Forschungsgemeinschaft (DFG 436 UKR/113/47/0-1), Slovak Grant Agency for Science (Project No 2/1134/21), and the DAAD-German Academic Exchange Service (PPP Slovakia 2002/2003).

REFERENCES

1. N. B. Dahotre, P. Kadolkar, S. Shah. *Surf. Interface Anal.* **31**, 659 (2001).
2. A. I. Y. Tok, F. Y. C. Boey, K. A. Khor. *Proc. Fabric. Advanced Materials* **VI**, 1791 (1998).
3. J. A. Owczarek and F. L. Howland. *IEEE* **13**, 358 (1990).
4. D. E. Riemer. *Solid State Tech.* **85**, 107, parts I/II (1988).
5. J. Pan, G. L. Tonkay, A. Quintero. *International Symposium on Microelectronics* 264 (1998).
6. M. Schieber. *J. Cryst. Growth* **109**, 401 (1991).

7. J. Blaich, K. H. Gillardon, G. Keser, L. Landt, G. Mayer, W. Schal. *Handwerk und Technik* **244** (1995).
8. E. H. Lutz. *PMI (Powder Metallurgy Int.)* **25**, 131 (1993).
9. M. Ueltzen, H. Altenburg, Ch. Seega, D. Litzkendorf, F. Fischer, P. Görnert. *EUCAS* **148**, 179 (1995).
10. H. Altenburg, J. Plewa, W. Schultze, T. Vilics. BMBF-Forschungsbericht, VDI (2001).
11. D. Segal. Cambridge Univ. Press (1990).
12. J. Reed. *Principles of Ceramics Processing*, John Wiley, New York (1999).
13. H. Altenburg, W. Abmus, P. Droste, H. Eickenbusch, J. Plewa, M. Ueltzen. *Fortschrittberichte VDI 5/346* (1994).
14. H. J. Scheel, M. Berkowski, B. Chabot. *J. Cryst. Growth* **115**, 19 (1991).
15. A. M. John, R. Jose, J. Kurian, P. K. Sajith, J. Koshy. *J. Am. Ceram. Soc.* **82**, 1421 (1999).
16. P. Reynen. *Mater. Sci. Res.* **13**, 355 (1987).
17. P.-Y. Chu and R. C. Buchanan. *J. Mater. Res.* **9**, 844 (1994).
18. A. Ikegami, H. Arima, H. Tosaki, Y. Matsuoka, M. Ai, H. Minorikawa, Y. Asahino. *IEEE Trans. Comp., Hybrids, Manuf. Technol.* **4**, 541 (1980).
19. O. Shpotyuk, A. Kovalskiy, O. Mrooz, L. Shpotyuk, V. Pekhnyo, S. Volkov. *J. Eur. Ceram. Soc.* **21**, 2067 (2001).
20. M. Vakiv, O. Shpotyuk, O. Mrooz, I. Hadzaman. *J. Eur. Ceram. Soc.* **21**, 1783 (2001).
21. N. McN. Alford, S. J. Penn, T. W. Button. *Supercond. Sci. Technol.* **10**, 169 (1997).
22. R. Rangel, D. H. Galvan, G. A. Hirata, E. Adem, F. Morales. *Supercond. Sci. Technol.* **12**, 264 (1999).
23. J. Langhorn, Y. J. Bi, J. S. Abell. *Physica C* **271**, 164 (1996).
24. N. J. C. Ingle, D. A. Cardwell, A. R. Jones, F. Wellhofer, T. W. Button. *Supercond. Sci. Technol.* **8**, 282 (1995).
25. J. Langhorn and P. J. McGinn. *Supercond. Sci. Technol.* **12**, 337 (1999).
26. D. L. Schulz, P. A. Parilla, H. Gopalaswamy, A. Swartzlander, A. Duda, R. D. Blaugher, D. S. Ginley. *Mater. Res. Bull.* **30**, 689 (1995).
27. E. Ban, Y. Matsuoka, T. Yoshimura, K. Takahashi. *Thin Solid Films* **338**, 118 (1999).
28. Y. Matsuoka and E. Ban. *J. Alloys Compd.* **268**, 226 (1998).
29. M. Jergel, Š. Chromik, V. Štrbik, V. Šmatko, F. Hanic, G. Plesch, Š. Buchta, S. Valtyniova. *Supercond. Sci. Technol.* **5**, 225 (1992).
30. J. L. MacManus-Driscoll, A. Ferreri, J. J. Wells, J. G. A. Nelstrop. *Supercond. Sci. Technol.* **14**, 96 (2001).
31. S. Sathyamurthy and K. Salama. *Physica C* **329**, 58 (2000).
32. J. Kurian, S. P. Pai, P. K. Sajith, K. V. O. Nair, K. S. Kumar, J. Koshy. *Physica C* **316**, 107 (1999).
33. M. Vasyuk, I. Lasaryuk, M. Matvijiv, H. Altenburg, J. Plewa. *Visnyk Lviv Univ. Phys. Series* **33**, 173 (2000).
34. J. Plewa, R. Lutcv, M. Vasyuk, I. Solski, V. Vashook, O. Tolochko, N. Munser, H. Altenburg. *EUCAS* 266 (2001).
35. J. Keller. *EUCAS C3*, 105 (2001).
36. H. Noji and A. Oata. *Supercond. Sci. Technol.* **5**, 269 (1992).
37. H. B. Liu, P. J. Ferreira, J. B. Vander Sande, A. Otto. *Physica C* **316**, 234 (1999).
38. T. Nasegawa, T. Koizumi, N. Ohtani, H. Kitaguchi, H. Kumakura, K. Togano, H. Miao. *Supercond. Sci. Technol.* **13**, 23 (2000).
39. H. Kitaguchi, K. Itoh, T. Takeuchi, K. Kumakura, H. Miao, H. Wada, K. Togano, T. Hasegawa, T. Koizumi. *Physica C* **320**, 253 (1999).
40. D. Buhl, T. Lang, L. J. Gauckler. *Supercond. Sci. Technol.* **10**, 32 (1997).
41. Th. Lang, D. Buhl, L. J. Gauckler. *Physica C* **294**, 7 (1998).
42. H. B. Liu, P. J. Ferreira, J. B. Vander Sande. *Physica C* **316**, 261 (1999).

43. St. Köbel. Ph.D. dissertation, ETH Zurich, 14090 (2001).
44. B. A. Glowacki. *Supercond. Sci. Technol.* **13**, 584 (2000).
45. J. I. Shimoyama, K. Kadowaki, H. Kitaguchi, H. Kumakura, K. Togano, H. Maeda, K. Nomura. *Appl. Supercond.* **1**, 43 (1993).
46. R. Funahashi, I. Matsubara, O. Ogura, K. Ueno, H. Ishikawa. *Physica S* **273**, 337 (1997).
47. S. L. Huang and D. New-Hughes. *Physica C* **319**, 104 (1999).
48. M. Jergel, A. Conde Gallardo, C. Falcony Guajardo, V. Štrbík. *Supercond. Sci. Technol.* **9**, 427 (1996).
49. R. T. Kampwirth, J. G. Hu, J. D. Hettinger, J. D. Miller, K. E. Gray, J. A. DeLuca. *IEEE Trans. Appl. Supercond.* **5**, 1954 (1995).
50. O. Heimpl, W. T. König, G. Gritzner. *Supercond. Sci. Technol.* **13**, 391 (2000).
51. S. Lee, N. P. Kiryakov, D. A. Emelyanov, M. S. Kuznetsov, Yu. D. Tretyakov, V. V. Petrykin, M. Kakihana, H. Yamauchi, Yi Zhuo, Mun-Seog Kim, Sung-Ik Lee. *Physica C* **305**, 57 (1998).
52. S. H. Su, P. V. P. S. S. Sastry, J. Schwartz. *Physica C* **361**, 292 (2001).
53. R. N. Bhattacharya, M. Feldmann, D. Larbalestier, R. D. Blaugher. *IEEE Trans. Appl. Supercond.* **11**, 3102 (2001).
54. E. Bellingeri, H. L. Suo, J. Y. Genoud, M. Schindl, E. Walker, R. Flükiger. *IEEE Trans. Appl. Supercond.* **11**, 3122 (2001).
55. Y. Tsabba and S. Reich. *Physica C* **254**, 21 (1995).
56. A. Sin, F. Weiss, P. Odier, Z. I. Supardi, M. Nunez-Regueiro. *Physica C* **341**, 399 (2000).
57. A. Mogro-Campero, P. J. Bednarczyk, Y. Gao, R. B. Bolon, J. E. Tkaczyk, J. A. DeLuca. *Physica C* **269**, 325 (1996).